

Microscopic nature of the photon strength function: stable and unstable Ni and Sn isotopes

Oleg Achakovskiy¹, Alexander Avdeenkov¹, Stephane Goriely², Sergei Kamedzhiev^{3,a}, Siegfried Krewald⁴, and Dmitriy Voitenkov¹

¹*Institute for Physics and Power Engineering, 249033 Obninsk, Russia*

²*Institut d'Astronomie et d'Astrophysique, ULB, CP226, B1050, Brussels, Belgium*

³*Institute for Nuclear Power Engineering NRNU MEPhI, 249040 Obninsk, Russia*

⁴*Institut fuer Kernphysik, Forschungszentrum Juelich, D-52425 Juelich, Germany*

Abstract. The pygmy-dipole resonances and photon strength functions in stable and unstable Ni and Sn isotopes are calculated within the microscopic self-consistent version of the extended theory of finite fermi systems which includes the QRPA and phonon coupling effects and uses the known Skyrme forces SLy4. The pygmy dipole resonance in ⁷²Ni is predicted with the mean energy of 12.4 MeV and the energy-weighted sum rule exhausting 25.6% of the total strength. The microscopically obtained photon E1 strength functions are used to calculate nuclear reaction properties, i.e the radiative neutron capture cross section, gamma-ray spectra, and average radiative widths. Our main conclusion is that in all these quantities it is necessary to take the phonon coupling effects into account.

1 Introduction

During the last decade there has been an increasing interest in the description of the Pygmy Dipole Resonance (PDR) manifested both in “pure” low-energy nuclear physics [1, 2] and in the nuclear data field [3–5]. Usually the PDR is considered in the energy region between zero and near the separation neutron energy and exhausts typically about 1-2% of the Energy Weighted Sum Rule (EWSR) but in neutron-rich nuclei, for example ⁶⁸Ni and probably ⁷²Ni, ⁷⁴Ni, this fraction is much larger. It is also necessary to note that for nuclei with small neutron separation energy, i.e less than 3-4 MeV, the PDR properties significantly change [3], and therefore phenomenological systematics obtained by fitting characteristics of stable nuclei (with a separation energy of about 8 MeV) is not suitable. In this sense, phenomenological approaches have no predictive strength and should not be used for applications in nuclear astrophysics. For these reasons, the microscopic self-consistent approaches, which pretend (ideally) to describe the ground and excited states of all nuclei using a small number of universal parameters like Skyrme interactions or energy density functionals, have been developed very actively [2, 3].

As a rule, in the nuclear data field, only phenomenological models for PDR and photon strength functions (PSF), based on various improvements of the Lorentzian-type approximation, are used (see, in particular, the Reference Input Parameters Libraries, known as RIPL) [4, 5]. However, as it was noted in RIPL2 and RIPL3 [4, 5],

the phenomenological Lorentzian-based expressions for PSF suffer from various shortcomings: in particular, “they are unable to predict the resonance-like enhancement of the E1 strength at energies below the neutron separation energy” and “this approach lacks reliability when dealing with exotic nuclei.” For these reasons, since 2006, the microscopic self-consistent PSF calculated within the Hartree-Fock-Bogolyubov method and Quasiparticle Random Phase Approximation (HFB+QRPA) have been included in RIPL2 [4], RIPL3 [5] and in modern nuclear reaction codes like EMPIRE and TALYS. In general, such an approach is very natural because it uses the single-particle properties of each nucleus and is therefore of higher predictive power for the exotic ones in comparison with phenomenological models. However, as we discuss below and as confirmed by modern experiments, the HFB+QRPA approach is necessary but not sufficient. To be exact, it should be complemented by the effect describing the interaction of single-particle degrees of freedom with the phonon degrees of freedom, known as the phonon coupling (PC).

Recent experiments in the PDR energy region have given new information about the PDR and PSF structures. First, the PDR in the unstable neutron-rich ⁶⁸Ni has been found [6] at about 11 MeV, which is higher than the neutron threshold $B_n = 7.8$ MeV, and exhausts about 5% of the EWSR. Such a measurement was confirmed recently in Ref. [7]. Second, experiments on ⁸⁶Kr [8], Sn isotopes [9, 10] and other nuclei clearly show the resonance-like structures in the PSF and photo-absorption cross section, which cannot be explained within the Lorentzian ap-

^ae-mail: kaeve@obninsk.com

proach. Using the known Oslo method, the authors [9] found out that, in order to explain the observed enhancement of the PSF at $E > 5$ MeV with respect to the Generalized Lorentzian description, it is necessary to add a peak structure centered around 8-9 MeV with a strength covering about 2% of the EWSR. These structures were explained phenomenologically by including some additional strength, on top of the HFB+QRPA predictions, located at a centroid energy of 8.0-8.5 MeV and a strength corresponding to about 1% of the EWSR [10]. This fact directly confirms the necessity to improve the HFB+QRPA predictions and search for new sources of additional strength. In particular, the PC effects may be at the origin of such an extra strength, as discussed in Refs.[2, 11]. In our recent article [12], the self-consistent version of the extended theory of finite fermi systems (ETFFS) [11], in the quasi-particle time blocking approximation (QTBA) [13] has been used to calculate the standard strength functions for many stable and unstable Sn even-even isotopes. This QTBA model includes self-consistently the QRPA, phonon coupling and uses a discretized single-particle continuum.

In the present work, we use the same theoretical approach to calculate the PSF in the stable and unstable Ni and Sn isotopes in order : *i*) to describe the PDR in ^{68}Ni , predict it in ^{72}Ni and compare it with the stable ^{58}Ni isotope, *ii*) to calculate microscopically appropriate PSF and to use them in the reaction code to estimate various nuclear reaction properties, *iii*) to investigate the PC contribution to all these quantities.

2 PSF and PDR in Ni isotopes

In all ETFFS calculations, the standard strength function $S(\omega) = \frac{dB(E;ML)}{dE}$ is calculated. It determines the E1 photoabsorption cross section $\sigma(\omega) = 4.022\omega S(\omega)$ [11], where the photon energy ω is taken in MeV, S is in $\text{fm}^2\text{MeV}^{-1}$, and σ is in mb. The PSF is connected to $S(\omega)$ by the simple relation

$$f(E1) = \frac{1}{3(\pi\hbar c)^2} \frac{\sigma(\omega)}{\omega} = 3.487 \cdot 10^{-7} S(\omega), \quad (1)$$

where S is expressed in $\text{fm}^2\text{MeV}^{-1}$ and $f(E1)$ in MeV^{-3} .

In the present study, we use the SLy4 Skyrme force. The ground state is calculated within the HFB method using the spherical code HFBRAD [14]. The residual interaction for the (Q)RPA and QTBA calculations is derived as the second derivative of the Skyrme functional. Our smoothing parameter is 200 keV.

In Fig. 1, we show six phenomenological models for the E1 PSF [4] of ^{120}Sn , and compare them with our microscopic QRPA and QTBA, i.e. QRPA + PC, results. In Figs. 2 and 3, the E1 PSF are shown together with the phenomenological EGLO model [4] for ^{68}Ni and ^{116}Sn , respectively. It can be seen that: 1) in contrast to phenomenological models, in the Sn and Ni nuclei, structure patterns caused by both the QRPA and PC effects can be observed, the latter ones being noticeably lower than the QRPA ones at $E < 10$ MeV for Sn isotopes, 2) a good

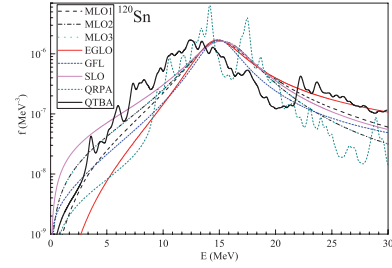


Figure 1. E1 PSF for ^{120}Sn . Six phenomenological variants from RIPL2 are shown. Dotted line: selfconsistent QRPA. Full line: QTBA (final results with PC)

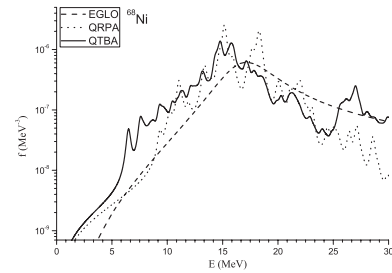


Figure 2. E1 PSF for ^{68}Ni . Dotted line: selfconsistent QRPA. Full line: QTBA (final results with PC). Dashed line : Enhanced Generalized Lorentzian (EGLO) model [4]

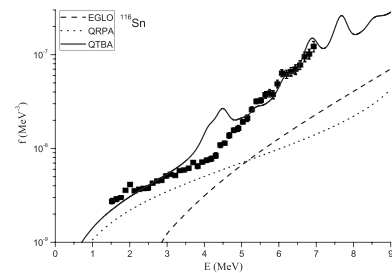


Figure 3. Same as in Fig.2 but for ^{116}Sn . Experiment are taken from Ref. [9]

agreement is found with experiment [9] for ^{116}Sn thanks to the inclusion of the PC (Fig. 3).

In Table 1, the integral parameters of the PDR in three Ni isotopes are given for three PSF models, i.e. the phenomenological EGLO, our microscopic QRPA and QTBA (QRPA+PC). For comparison, the 6 MeV interval where the PDR was observed in ^{68}Ni is considered. In this interval, the PDR characteristics have been approximated, as usual, with a Lorentz curve by fitting the three moments of the Lorentzian and theoretical curves [11]. A reasonable agreement with experimental data [6, 7] is obtained. Earlier, a similar calculation was performed for ^{68}Ni [15] using the relativistic QTBA, with two phonon contributions additionally taking into account. Concomitantly, the PDR characteristics in ^{72}Ni have been estimated leading in this interval to a mean energy of 12.4 MeV and the large strength of 25.7% of the total EWSR. In all the isotopes, large PC contribution to the PDR strength is found.

Table 1. Integral characteristics of the PDR in Ni isotopes calculated in the (8-14) MeV interval for ^{58}Ni , ^{72}Ni and (7-13) MeV interval for ^{68}Ni (see text for details).

Nuclei	EGLO		QRPA		QTBA	
	E, MeV	%	E, MeV	%	E, MeV	%
^{58}Ni	11.3	2.4	13.3	6	14.0	11.7
^{68}Ni	11.3	3.1	11.0	4.9	10.8	8.7
^{72}Ni	11.3	3.4	12.4	14.7	12.4	25.7

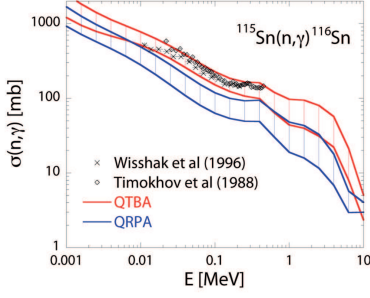


Figure 4. $^{115}\text{Sn}(n,\gamma)$ cross section calculated with the QRPA (blue) and QTBA (red) PSF. The uncertainty bands depict the uncertainties affecting the nuclear level density predictions [16–18]. Experimental cross section are taken from Refs. [19, 20]

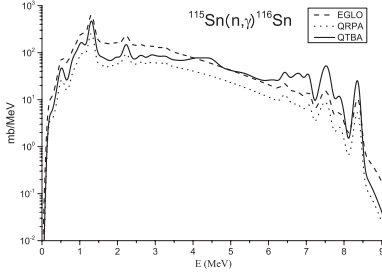


Figure 5. Gamma-ray spectra from $^{115}\text{Sn}(n,\gamma)$ for the neutron energy of 100 keV

3 Neutron radiative capture

In Fig. 4, the radiative neutron capture cross section for the ^{115}Sn obtained with the QRPA and QRPA+PS photon E1 strength functions is shown. We also show the uncertainty bands obtained when considering various nuclear level density models [16–18]. One can see clearly that the agreement with experiment is possible only when the PC is taken into account.

The corresponding capture gamma-ray spectra calculated for the neutron energy of 100 keV are given in Fig. 5 and compared with the result obtained with the EGLO PSF model. Here the phenomenological Generalized Superfluid model [4] of nuclear level densities is adopted. On the whole, our results are in an agreement with the EGLO ones (for this stable nucleus) and show that the PC contribution is significant. For all three variants some structures are found. Unfortunately, no experimental data exist for this case.

4 Average radiative widths

Average radiative widths of neutron resonances Γ_γ are very important properties of gamma-decay from high-energy nuclear states; they are used in nuclear reaction calculations, in particular to normalise the γ -ray strength. There are a lot of experimental data for them [21, 22]. For 11 Sn and Ni isotopes, we have calculated the widely used quantity $2\pi\Gamma_\gamma/D_0$ with the EGLO and our QRPA and QTBA PSF models and the GSM nuclear level density model [4] for the s-wave spacing D_0 (Table 2). As far as we know, these are the first calculations performed with PC. We found that, except for ^{68}Ni , the PC increases the QRPA contribution by 100–200% in the direction of the systematics. The results for ^{120}Sn and ^{62}Ni , for which experimental data (not systematics) exists, are of great interest. Here we obtain a good agreement with experiment, which probably means that the M1 contribution is not large (especially for ^{120}Sn). As far as the EGLO model is concerned, it is clear that the predictions differ from the systematics [21] and experimental data (and also from our QTBA results) rather strongly.

Table 2. Quantities $2\pi\Gamma_\gamma/D_0$ for s-neutrons where Γ_γ is the average radiative width (see text for details). The experimental data (underlined) and systematics are taken from [22] and [21], respectively.

Nuclei	EGLO	QRPA	QTBA	exp. or system.
^{110}Sn	$12.6 \cdot 10^{-2}$	$3.90 \cdot 10^{-2}$	$7.99 \cdot 10^{-2}$	$9.57 \cdot 10^{-2}$
^{112}Sn	$9.44 \cdot 10^{-2}$	$3.08 \cdot 10^{-2}$	$5.88 \cdot 10^{-2}$	$9.76 \cdot 10^{-2}$
^{116}Sn	$7.99 \cdot 10^{-3}$	$3.33 \cdot 10^{-3}$	$5.79 \cdot 10^{-3}$	$11.73 \cdot 10^{-3}$
^{120}Sn	$5.77 \cdot 10^{-3}$	$2.52 \cdot 10^{-3}$	$7.10 \cdot 10^{-3}$	<u>$6.98 \cdot 10^{-3}$</u>
^{124}Sn	$4.77 \cdot 10^{-3}$	$2.13 \cdot 10^{-3}$	$2.67 \cdot 10^{-3}$	$9.84 \cdot 10^{-3}$
^{132}Sn	$6.53 \cdot 10^{-4}$	$2.18 \cdot 10^{-4}$	$2.42 \cdot 10^{-4}$	$1.39 \cdot 10^{-4}$
^{136}Sn	$9.90 \cdot 10^{-7}$	$9.97 \cdot 10^{-7}$	$1.10 \cdot 10^{-6}$	$6.51 \cdot 10^{-6}$
^{58}Ni	$7.04 \cdot 10^{-3}$	$2.30 \cdot 10^{-3}$	$7.33 \cdot 10^{-3}$	$17.0 \cdot 10^{-3}$
^{62}Ni	$2.51 \cdot 10^{-3}$	$1.97 \cdot 10^{-3}$	$4.33 \cdot 10^{-3}$	<u>$5.98 \cdot 10^{-3}$</u>
^{68}Ni	$1.04 \cdot 10^{-4}$	$4.73 \cdot 10^{-5}$	$2.46 \cdot 10^{-4}$	$2.64 \cdot 10^{-4}$
^{72}Ni	$5.08 \cdot 10^{-5}$	$1.33 \cdot 10^{-5}$	$2.45 \cdot 10^{-5}$	$5.08 \cdot 10^{-5}$

5 Conclusion

The characteristics of nuclear reactions with gamma-rays have been calculated within the microscopic self-consistent approach which takes into account the QRPA and PC effects and uses the SLy4 Skyrme force. Such a self-consistent approach is of particular relevance for nuclear astrophysics. A reasonable agreement with experiment has been obtained for the PSF in ^{116}Sn and the PDR integral properties in ^{68}Ni . We predict the PDR in the spherical ^{72}Ni nucleus at 12.4 MeV with a very large strength corresponding to 25.7% of the EWSR. For the first time, the average radiative widths have been calculated microscopically with the PC taken into account. In all the considered quantities, the contribution of PC turned out to be significant. These results confirm the necessity to include the PC effects into the theory of nuclear data both for stable and unstable nuclei.

S. Kamerdzhev acknowledges the CGS15 Organizing Committee and Prof. R. Schwengner for the invitation and support, Drs. V. Furman and A. Sukhovoij for discussions of the results.

References

- [1] D. Savran, T. Aumann, A. Zilges, *Prog. Part. Nucl. Phys.* **70**, 210 (2013).
- [2] N. Paar, D. Vretenar, E. Khan, G. Colo, *Rep. Prog. Phys.* **70**, 691 (2007).
- [3] S. Goriely, E. Khan, M. Samyn, *Nucl. Phys. A* **739**, 331 (2004).
- [4] *Reference Input Parameter Library, RIPL-2*, IAEA-TECDOC-1506. See also <https://www-nds.iaea.org/RIPL-2> (2006).
- [5] R. Capote, *et al.*, *Nuclear Data Sheets* **110**, 3107 (2009). See also <https://www-nds.iaea.org/RIPL-3>.
- [6] O. Wieland, *et al.*, *Phys. Rev. Lett.* **102**, 092502 (2009).
- [7] D. M. Rossi, *et al.*, arXiv:1209.1024 (2012).
- [8] R. Schwengner, R. Massarczyk, G. Rusev *et al.*, *Phys. Rev. C* **87**, 024306 (2013).
- [9] H.K. Toft, *et al.*, *Phys. Rev. C* **83**, 044320 (2011).
- [10] H. Utsunomiya, *et al.*, *Phys. Rev. C* **84**, 055805 (2011).
- [11] S. Kamerdzhev, J. Speth, G. Tertychny, *Phys. Rep.* **393**, 1 (2004).
- [12] A. Avdeenkov, S. Goriely, S. Kamerdzhev, S. Krewald, *Phys. Rev. C* **83**, 064316 (2011).
- [13] V. Tselyaev, *Phys. Rev. C* **75**, 024306 (2007).
- [14] K. Bennaceur and J. Dobaczewski, *Comp. Phys. Comm.* **168**, 96 (2005).
- [15] E. Litvinova, P. Ring, V. Tselyaev, *Phys. Rev. Lett.* **105**, 022502 (2010).
- [16] S. Goriely, S. Hilaire, A.J. Koning, *Phys. Rev. C* **78**, 064307 (2008).
- [17] A.J. Koning, S. Hilaire, S. Goriely *Nucl. Phys. A* **810**, 13 (2008).
- [18] S. Hilaire, M. Girod, S. Goriely, A.J. Koning, *Phys. Rev. C* **86**, 064317 (2012).
- [19] K. Wisshak, *et al.*, *Phys. Rev. C* **54**, 1451 (1996).
- [20] V.M. Timokhov, *et al.* *Fiz.-Energ Institut, Obninsk Reports No.1921* (1988).
- [21] *Reference Input Parameter Library, RIPL-1*, IAEA-TECDOC-1034 (1998).
- [22] S.F. Mughabghab, *Atlas of neutron Resonances, Resonance Parameters and Thermal Cross Sections Z=1-100* (Elsevier, Amsterdam, 2006).